Published in final edited form as:
Mol Cell Neurosci. 2011 June ; 47(2): 71–78. doi:10.1016/j.mcn.2010.10.002.

Dominant Cx26 mutants associated with hearing loss have dominant-negative effects on wild type Cx26

Junxian Zhang[1], **Steven S. Scherer**[2], and **Sabrina W. Yum**[1,2]

[1]Division of Neurology, The Children's Hospital of Philadelphia, University of Pennsylvania, Philadelphia, PA 19104

[2]Department of Neurology, University of Pennsylvania, Philadelphia, PA 19104

Abstract

Mutations in *GJB2*, the gene encoding the human gap junction protein connexin26 (Cx26), cause either non-syndromic hearing loss or syndromes affecting both hearing and skin. We have investigated whether dominant Cx26 mutants can interact physically with wild type Cx26. HeLa cells stably expressing wild type Cx26 were transiently transfected to co-express nine individual dominant Cx26 mutants; six associated with non-syndromic hearing loss (W44C, W44S, R143Q, D179N, R184Q, and C202F) and three associated with hearing loss and palmoplantar keratoderma (G59A, R75Q, and R75W). All mutants co-localized and co-immunoprecipitated with wild type Cx26, indicating that they interact physically, likely by forming admixed heteromeric/heterotypic channels. Furthermore, all nine mutants inhibited the transfer of calcein in cells stably expressing Cx26, demonstrating that they each have dominant effects on wild type Cx26. Taken together, these results show that dominant-negative effects of these Cx26 mutants likely contribute to the pathogenesis of hearing loss.

Keywords

gap junctions; hearing; FRAP; immunoprecipitation; dye transfer; cochlea; disease mechanism

INTRODUCTION

Gap junctions (GJs) are intercellular channels that allow the direct passage of ions and small molecules (typically < 1000 Da) between adjacent cells, and are thought to have diverse functions, including the propagation of electrical signals, metabolic cooperation, spatial buffering of ions, growth control, and cellular differentiation (Bruzzone et al., 1996). A complete channel is formed when one hemichannel (or connexon) docks with a compatible hemichannel on an apposed cell membrane; each hemichannel is comprised of six compatible connexin molecules - a large family of highly conserved proteins, named according to their predicted molecular mass (Willecke et al., 2002). Individual hemichannels can be composed of one (homomeric) or more than one (heteromeric) type of connexins.

Address for correspondence: Sabrina W. Yum, M.D., Division of Neurology, Children's Hospital of Philadelphia, Abramson Research Center, Room 502A, 34th Street and Civic Center Boulevard, Philadelphia, PA 19104, Phone: 215-590-1719, FAX: 215-590-1771, yums@email.chop.edu.

Similarly, channels can be composed of hemichannels comprised of the same (homotypic) or different (heterotypic) connexins (Kumar and Gilula, 1996; White and Bruzzone, 1996). The configuration and molecular composition of channels affect the biophysical properties such as permeability and gating (Harris, 2001).

Mutations in *GJB2*, *GJB6*, and *GJB3*, the genes that encode the human gap junction proteins connexin26 (Cx26), Cx30, and Cx31, respectively, cause hearing loss (Estivill et al., 1998; Grifa et al., 1999; Kelsell et al., 1997; Xia et al., 1998). Recessive mutations of *GJB2* are the most common cause of hereditary non-syndromic hearing loss, accounting for up to 50% of such patients, with over 90 recessive mutations reported (http://davinci.crg.es/deafness/). At least 30 dominant mutations in *GJB2* have also been reported to cause hearing loss, either in isolation (non-syndromic) or as part of a syndrome with various skin disorders, including palmoplantar keratoderma (PPK). Recessive *GJB2* mutations likely cause simple loss of function, whereas dominant *GJB2* mutations likely cause gain of function, including dominant-negative effects on wild type (WT) Cx26 and/or Cx30 (Marziano et al., 2003; Yum et al., 2010).

Cx26 is widely expressed throughout non-sensory epithelial and connective tissue cells, and is largely co-expressed with Cx30 in the inner ear (Ahmad et al., 2003; Forge et al., 2002; Jagger and Forge, 2006; Kikuchi et al., 1995; Lautermann et al., 1998; Sun et al., 2005). We reported that 9 dominant Cx26 mutants co-immunoprecipitated with Cx30, indicating that they form admixed heteromeric/heterotypic channels and 8 of them have trans-dominant effects on Cx30 (Yum et al., 2010). Cx26 mutants are proposed to exert their dominant-negative effect on WT Cx26 by forming heteromeric/heterotypic channels as well (Marziano et al., 2003; Oshima et al., 2003; Piazza et al., 2005), but this has not been directly demonstrated. In this study, we extended the analysis of these nine dominant Cx26 mutants (Suppl. Fig. 1) - six (W44C, W44S, R143Q, D179N, R184Q and C202F) that cause non-syndromic hearing loss (NSHL) and three (G59A, R75Q and R75W) that cause syndromic hearing loss (SHL) associated with PPK, and demonstrated that all nine co-localized and co-immunoprecipitated with WT Cx26, indicating that these individual mutants co-assembled with WT Cx26 into heteromeric/heterotypic channels, and they either partially or completely inhibited dye transfer of WT Cx26. Dominant-negative effects of these Cx26 mutants likely contribute to the pathogenesis of hearing loss.

MATERIALS AND METHODS

Chimeric/epitope tagged Cx26 and mutant Cx26 expression constructs

A plasmid containing human *GJB2* (kindly provided by Dr. Bruce Nicholson) was amplified by PCR using oligonucleotide primers designed to include the open reading frame (ORF) and incorporate a 5' *NheI* site and a 3' *BamHI* site. The PCR product was ligated into pIRESneo3 and/or pIRESpuro3 (Clontech, Palo Alto, CA), and the pIRES2-DsRed bicistronic vector (Orthmann-Murphy et al., 2007) as previously described (Yum et al., 2007). The *GJB2* mutations were introduced into the ORF of human *GJB2* cDNA by PCR site-directed mutagenesis using the QuickChange kit (Stratagene, La Jolla, CA). To generate the mutations, oligonucleotide mutagenic primers were designed and incorporated using *Pfu-Turbo* DNA polymerase. The PCR products were digested by *Dpn*I endonuclease to eliminate the parental DNA template. The resulting DNA was used to transform XL-1 Blue bacteria, and minipreps were made from single colonies and sequenced at the Cell Center at the University of Pennsylvania. A large-scale plasmid preparation was made from a single colony (Qiagen) and the *GJB2* sequence and each mutation was confirmed by direct sequencing.

To generate fusion proteins of Cx26 and EGFP (Cx26EGFP) and DsRed (Cx26DsRed), human *GJB2* cDNA was amplified by PCR using oligonucleotide primers designed to include the ORF, delete the stop codon and incorporate a 5' *EcoRI* site and a 3' *BamHI* site, using *Pfu* Turbo polymerase. The PCR products were cloned into the *EcoRI* and the *BamHI* restriction sites of vector pEGFPN1 or DsRed-monomer-N1 (Clontech, Palo Alto, CA). The resulting constructs have *GJB2* in frame with EGFP or DsRed with a 7 amino acid linker. To generate fusion proteins of Cx26 and V5 (Cx26V5), myc (Cx26Myc), and FLAG (Cx26FLAG), an adaptor-duplex containing each epitope tag sequence, a 5' *BamHI* site, and a 3' *BsrGI* site was synthesized, and subcloned into the 5' *BamHI* and the 3' *BsrGI* restriction sites of the Cx26EGFP construct, replacing the EGFP sequence with that of the specific epitope tag. The resulting constructs were sequencing from a large-scale plasmid preparation obtained from a single colony.

Generating cell lines expressing WT Cx26 or Cx26 mutants

Communication-incompetent HeLa cells (Elfgang et al., 1995) were obtained from Dr. Klaus Willecke. They were grown in low-glucose Dulbecco's modified Eagle's Medium (DMEM) supplemented by 10% fetal bovine serum (FBS) and antibiotics (100 units/ml penicillin, 100 μg/ml streptomycin) in a humidified atmosphere containing 5% CO_2 at 37°C. To generate transiently transfected cells, HeLa cells were grown on coverslips in 24 well plates, and transfection with FuGENE 6 transfection reagent (Roche Applied Science, Indianapolis, IN) according to the manufacturer's protocol. Briefly, FuGENE 6 was diluted in Opti-MEM (GIBCO BRL, Carlsbad, California), then admixed with plasmids encoding Cx26V5, Cx26Flag, Cx26Myc, Cx26DsRed, Cx26EGFP, WT Cx26 or individual Cx26 mutations, or equal amounts of plasmids encoding Cx26V5 and (untagged), WT Cx26, or individual human Cx26 mutations in the co-transfection experiments. The transfection reagent:DNA complex was incubated for 15–20 min at RT, then added to HeLa cells (approximately 50% confluent), incubated for 2 days in DMEM at 37°. Immunostaining, immunoblot analysis or co-immunoprecipitation experiments were performed two days after transfection.

Immunocytochemistry

HeLa cells were grown on coverslips for 2 days to approximately 70–80% confluence, washed in 1X PBS, fixed in acetone at −20°C for 10 min, blocked (5% fish skin gelatin in 1X PBS containing 0.1% Triton) for 1 hr in RT, and incubated overnight at 4°C with various antibodies diluted in blocking solution. After washing in PBS, TRITC-conjugated donkey anti-rabbit, and FITC-conjugated donkey anti-mouse secondary antibodies were added in the same blocking solution (1:200) and incubated at RT for 1 hr. Coverslips were mounted with Vectashield (Vector Laboratories Inc., Burlingame, CA) and samples were photographed with a Leica fluorescence microscope with a Hamamatsu digital camera C4742-95 connected to a G5 Mac computer, using the Openlab 2.2 software for deconvolution. Confocal images were captured using a 60X, oil immersion objective on the Leica TCS SPZ AOBS confocal microscope system (USA). Z series were taken through the cells at near the limit of resolution. Three confocal planes near the middle of the z series that contain the sharpest images of cells were stacked using the ImageJ software and analyzed for the expression of both Cx26V5 and Cx26 mutants.

We used a monoclonal antibody (Zymed Laboratories 33-5800, South San Francisco, CA; diluted 1:500) and a rabbit antiserum (Zymed Laboratories 51-2800, South San Francisco, CA, diluted 1:1000) against the C-terminus of Cx26 (Cx26-C), a rabbit antiserum against the intracellular loop of Cx26 (Cx26-L; Zymed Laboratories 71-0500, South San Francisco, CA; diluted 1:1000), monoclonal antibodies against V5 (Invitrogen, Carlsbad, CA, diluted 1:1000), FLAG (Sigma-Aldrich, diluted 1:2000), or c-Myc (Sigma, diluted 1:1000), and

rabbit antisera against V5 (Sigma-Aldrich, diluted 1:1000), FLAG (Sigma, diluted 1:2000), or c-Myc (Sigma, diluted 1:1000). For cells co-expressing individual Cx26 mutants and Cx26V5, we typically used the combination of the rabbit antiserum against Cx26-C and the mouse monoclonal antibodies against V5 because we found that the epitope tag "blocks" the immunoreactivity of Cx26V5 to antibodies against Cx26-C (Fig. 1).

Immunoblot analysis and co-immunoprecipitations

For immunoblots, HeLa cells were grown to confluence on 100 mm plates, harvested in cold Dulbecco's PBS lacking Ca^{2+} and Mg^{2+} (Invitrogen, Carlsbad, CA). The supernatant was removed, the pellet was lysed in ice-cold lysis buffer (50 mM Tris, pH = 7.0, 1% dodesylsulfate (SDS), and 0.017 mg/ml phenylmethylsulfonyl fluoride (Sigma-Aldrich, St. Louis, MO), followed by a brief sonication (15 sec on, 10 sec off, for six times) on ice with a dismembrator (Fisher Scientific, Pittsburgh, PA). The protein concentration of each sample was measured (Bio-Rad Laboratories, Richmond, CA) according to manufacturer's instructions. 100 μg of each sample was incubated with electrophoresis buffer (62.5 mM Tris, pH = 6.8, 20% glycerol, 2% SDS, 100 mM DTT and bromophenol blue) at RT for 5–15 min, loaded onto 12% SDS-polyacrylamide gel, electrophoresed, transferred to an Immobilon-polyvinylidene fluoride membrane (Millipore, Billerica, MA) using a semi-dry transfer unit (Bio-Rad, Hercules, CA), blocked (5% blotting grade blocker non-fat dry milk and 0.5% Tween-20 in Tris-buffered saline) for 1 h, and incubated overnight at 4°C with various primary antibodies against Cx26 (diluted in blocking solution). The blots were washed in blocking solution, incubated in peroxidase-coupled donkey antiserum against rabbit or mouse IgG (Jackson ImmunoResearch, West Grove, PA, diluted 1:10,000) for 1 h at RT. After washing in blocking solution and Tris-buffered saline containing 0.5% Tween-20, the blots were visualized by enhanced chemiluminescence (Amersham, Piscataway, NJ) according to the manufacturer's protocol. In this way, we found that a rabbit antiserum against Cx26-C (Zymed Laboratories 51-2800, South San Francisco, CA) and a monoclonal antibody against Cx26-C (Zymed Laboratories 33-5800, South San Francisco, CA; diluted 1:500) did not bind to Cx26V5.

For co-immunoprecipitations, HeLa cells (grown on 60 mm plates) were transiently transfected to co-express Cx26V5 and (untagged) WT Cx26, a Cx26 mutant, or Cx43, lysed in 500 μL of ice-cold RIPA buffer (10 mM sodium phosphate pH 7.0, 150 mM NaCl, 2 mM EDTA, 50 mM sodium fluoride, 1% NP-40, 1% sodium deoxycholate, and 0.1% SDS) for 15 minutes on ice, scraped, then spun at 14,000 rpm for 30 minutes. The supernatants were collected, and incubated on ice with either 10 μl mouse monoclonal antibody against V5 (Invitrogen) or 5 μl rabbit antiserum against V5 (Sigma-Aldrich) for 1 hour. Protein G agarose (100 μl) was added to the above cell lysates/antibody solution, and incubated overnight at 4°C. The beads were washed in RIPA buffer, re-suspended in electrophoresis buffer (62.5 mM TRIS, 20% glycerol, 2% SDS, 100 mM DTT), separated on 12% SDS-polyacrylamide gel for protein detection following the immunoblotting protocol described. The blots were initially incubated with a rabbit polyclonal antiserum against Cx26-C or Cx43, respectively, visualized, and then re-hybridized with a rabbit antiserum against V5. The blots were stripped, then re-hybridized again with a rabbit antiserum against Cx26-L.

Fluorescence recovery after photobleaching (FRAP)

For FRAP, HeLa cells stably expressing Cx26 (Yum et al., 2007) were grown on 35/22 mm glass bottom dish (Warner Instruments, Hamden, CT) and transiently transfected with a pIRES2-DsRed bicistronic vector containing WT *GJB2* or selected *GJB2* mutations, using Lipofectamine LTX reagent (Invitrogen, Carlsbad, CA) according to the manufacturer's "one tube" protocol. About 40 h after transfection, the cells (about 70–90% confluent) were washed in 1X HBSS, incubated with Calcein-AM (1 μM; Biotium, Haywood, CA) in Opti-

MEM (Invitrogen, Carlsbad, CA) for 20 min, rinsed several times with 1X HBSS, and maintained in Opti-MEM at RT during the experiment. We used the interactive software of a FluoView FV1000 Olympus laser scanning confocal microscope that has a synchronized laser scanning system, in which one laser provides high resolution images while the second laser simultaneously stimulates. Using a 60x objective, individual DsRed-positive cells that were surrounded by at least 4 other transfected (DsRed positive) cells (ranged 4–7 depending on the size and the shape of the cells) were bleached by placing a cursor within the contour of the cell membrane, and photobleached for 600 ms with a 405 nm, 25 mW diode laser at full power. The aim was to bleach maximally the selected cells, without bleaching neighboring cells. The 488-nm line of a 30 mW Argon laser at 0.3% excitation power of this instrument was used to detect the green fluorescence signal during the entire recording. To measure FRAP, images were acquired before bleaching and every 10 seconds following bleaching for 400 seconds. A circular cursor (slightly smaller than the one used to bleach the cell) was placed in the center of the bleached cell, average fluorescence intensity within the circle was measured as mean pixel density and exported as Excel files. One unbleached cell in the same field was also monitored for fluorescence loss throughout the experiment. In addition, individual cells that were isolated from the rest of the cells were also bleached and monitored for recovery in each dish; no recovery was observed (data not shown). Using Microsoft Excel software, the fluorescence signal intensity immediately prior and immediately after photobleaching was normalize to 100% and 0% respectively. Recovery was calculated based on the fluorescence intensity in the photobleached cell at each time point relative to the fluorescence intensity of the same cell at the same region prior to the bleaching and expressed as percent recovery.

To determine whether FRAP of cells co-expressing Cx26 and individual Cx26 mutants differed from those of cells co-transfected with plasmids containing WT Cx26 (in a DsRed bicistronic vector), we conducted a statistical analysis applying a repeated measure nonlinear regression model with autocorrelated errors to model recovery curve for the transformed percentages over time (Proc Mixed in SAS software version 9.1). The test for difference between two group-specific mean curves (each curve is a specific cell line) was based on the test of significance of the two interaction parameters (the group-slope and the quadratic time interactions). The error terms were assumed to be autocorrelated to account for correlations among the responses across time within a given cell line (Yum et al., 2010; Yum et al., 2007). A p-value of < 0.05 was considered to be significant.

RESULTS

All nine dominant Cx26 mutants co-localized with WT Cx26 in the gap junction plaques

We have recently shown that nine dominant Cx26 dominant mutants (W44C, W44S, G59A, R75Q, R75W, R143Q, D179N, R184Q, C202F) form gap junction plaques at apposed cell borders, similar in appearance to those formed by WT Cx26 (Yum et al., 2010). To determine whether these dominant mutants can interact with WT Cx26, we added various tags (EGFP or DsRed, as well as V5, myc, or FLAG epitopes) to the C-terminus of WT Cx26. Immunostaining transiently transfected HeLa cells showed that WT Cx26 with a V5 tag (Cx26V5) had the most similar expression pattern to that of (untagged) WT Cx26 (Suppl. Fig. 2), and that the V5 tag “blocked” the staining of a rabbit antiserum against the C-terminus of Cx26 (RbaCx26-C) but not that of a rabbit antiserum against the cytoplasmic loop of Cx26 (RbαCx26-L), as shown in Figure 1A. This serendipitous finding allowed us to localize Cx26V5 (with MαV5) and untagged Cx26 (with RbαCx26-C) separately in HeLa cells expressing both of them (Fig. 1A). Using this approach, we found that WT Cx26 and each of the 9 dominant Cx26 mutants formed gap junction plaques at apposed cell borders, as in cells transfected to express the individual mutants alone at the same time (Fig. 1C), and were largely co-localized with Cx26V5 in gap junction plaques at apposed cell borders (Fig.

1B). We have performed the transfection at least 5 times for each mutant with similar results. Thus, none of the nine Cx26 mutants affected the trafficking and localization of WT Cx26.

Cx26V5 and Cx26 mutants co-immunoprecipitate

The co-localization of Cx26V5 and Cx26 mutants in co-transfected cells suggests that they form heteromeric hemichannels. To evaluate directly this possibility, we immunoprecipitated Cx26V5 with a mouse monoclonal antibody against V5, blotted the immunoprecipitates with the rabbit antiserum against the C-terminus of Cx26. As shown in Figure 2, WT Cx26 as well as all 9 different mutants co-immunoprecipitated with Cx26V5. In contrast, Cx43 does not co-immunoprecipitate with Cx26V5 (Fig. 2A, right panel), in keeping with the evidence that these two connexins do not interact in mammalian cells (Gemel et al., 2004; Yum et al., 2007). To validate our approach, we demonstrated directly that two different V5 antibodies co-immunoprecipitate Cx26V5, but do not immunoprecipitate WT Cx26 itself, and that the V5 epitope tag largely blocks the binding of the rabbit antiserum against the C-terminus of Cx26 (Suppl. Fig. 3). We performed these experiments three times with similar results, and conclude that the dominant Cx26 mutants likely interact physically with Cx26WT, probably by forming heteromers.

Functional analysis of cells expressing Cx26V5 and/or Cx26 mutants

To investigate whether these dominant Cx26 mutants affect the function of WT Cx26, we compared the fluorescence recovery after photobleaching (FRAP), a quantitative analysis of dye transfer over time, in HeLa cells stably expressing Cx26 (Yum et al., 2007) transiently transfected with a pIRES2-DsRed bicistronic vector containing WT *GJB2* or one of the nine *GJB2* mutations. After transfection, confluent monolayers of cells were incubated in calcein AM, which is cleaved within cells, yielding calcein, a small (623 Da; -4 charge) fluorescent molecule. The number of neighboring cells needed to surround an individual cells completely in the culture ranged from 4–7 depending on the size and the shape of the cells; fewer cells if they were larger or if they were relatively elongated. Therefore, we selected individual DsRed-positive cells that were in close contact with at least four other DsRed-positive cells for photobleaching. The images were acquired immediately before and after bleaching, and every 10 seconds thereafter for 400 seconds; examples are shown in Figure 3A. The fluorescence was measured as mean pixel density in the bleached cell in every image. We normalized the data for each cell, assigning the fluorescent signal present in each cell immediately prior to and immediately after photobleaching as 100% and 0%, respectively, so that the data from different cells could be pooled. As shown in Figure 3B, all 9 mutants significantly suppressed calcein transfer of WT Cx26 ($p < 0.0001$), although the D179N mutant had less severe inhibition comparing to other mutants ($p < 0.0001$).

DISCUSSION

To simulate the *in vivo* situation in patients with dominant *GJB2* mutations, where mutant and WT Cx26 subunits are co-expressed due to the heterozygous state of the mutations, we investigated the interaction between nine individual dominant Cx26 mutants and WT Cx26 in a model system. The lack of binding of antibodies against the C-terminus of Cx26 to Cx26V5 enabled us to distinguish WT Cx26 (Cx26V5) from the untagged Cx26 mutants. In this way, we showed that nine dominant Cx26 mutants interact directly with WT Cx26 – all mutants were co-localized and co-immunoprecipitated with Cx26V5. Furthermore, we used a novel adaptation of a FRAP assay to demonstrate directly that all nine mutants diminished the function of WT Cx26. Our results, taken together, provide the first comprehensive demonstration that dominant Cx26 mutants interact physically with, and have dominant effects upon, WT Cx26, likely by forming heteromeric/heterotypic channels.

All nine dominant Cx26 mutants interact physically with WT Cx26

Up to 30 different dominant mutations in *GJB2* have been reported; 10 are associated with non-syndromic hearing loss (NSHL), and the others cause syndromic hearing loss (SHL) with various skin diseases. In this study, we focused our investigation on mutants associated with NSHL or SHL associated with the milder form of skin disease PKK. We previously reported that these nine dominant Cx26 mutants formed gap junction plaques in transfected cells when expressed alone, or when co-expressed with Cx30, with which they were co-localized (Yum et al., 2010). We extended the analysis here by showing that these nine mutants were also colocalized with Cx26V5, forming normal-appearing gap junction plaques. Our findings are consistent with previous reports that W44S, G59A, G59A-EGFP, W75Q-EYFP, or R75W-GFP formed gap junction plaques at the cell borders in cells co-expressing WT Cx26 (Marziano et al., 2003; Oshima et al., 2003; Piazza et al., 2005), but some of these reports did not directly demonstrate that both mutants and WT Cx26 were present in these plaques (Marziano et al., 2003). It should be noted that Marziono et al. (Marziano et al., 2003) made the W44S, G59A, G59A-EGFP, R75W-GFP mutations in a rat cDNA (and co-expressed these with WT rat Cx26), and that the rat G59A did not form gap junction plaques when expressed alone, whereas we and others (Thomas et al., 2007; Thomas et al., 2004) found that the human G59A mutant did form gap junction plaques when expressed alone. Similarly, our result was also different from a recent report of trafficking defect of the R184Q mutant (Su et al.). Technical reasons could account for the discrepancy as Su et al used a complicated Tet-on system in the experiment. In addition, they used an EGFP tagged plasmid that could potentially affect the trafficking of the protein.

We also provided the first demonstration that these nine mutants co-immunoprecipitated with Cx26V5; this is strong evidence of a direct interaction. Based on our co-immunoprecipitations of Cx26 and Cx30 (Yum et al., 2010), the predominant interaction demonstrated by this assay between individual mutants and WT Cx26 is heteromeric (within hemichannels) rather than heterotypic (between apposed hemichannels). This interpretation is consistent with the finding that R75W-His and Cx26 are co-eluted in the hexamer fraction in cells co-expressing them (Oshima et al., 2003).

Dominant-negative effect of Cx26 mutants on WT Cx26

All nine dominant Cx26 mutants inhibited dye transfer of WT Cx26, thereby providing direct evidence that each mutant has a dominant-negative effect on WT Cx26. Because we used a DsRed bicistronic vector, we avoided the potentially confounding effect of epitope tags, which can potentially alter the biophysical properties of connexin channels (Bukauskas et al., 2001; Sullivan and Lo, 1995). Our results confirm and extend prior reports that W44S or R75W diminished dye transfer in cells co-expressing (rat) Cx26 (Marziano et al., 2003); R75W inhibited sulforhodamine transfer when co-expressed with WT Cx26-GFP, while C64S (a recessive mutation) did not (Oshima et al., 2003); R75GYFP suppressed LY transfer and electrical coupling in HeLa cells expressing Cx26 (Piazza et al., 2005); HBL-100 cells co-expressing (rat) Cx26 and either G59A-GFP or D66H-GFP exhibited an 80% decrease in dye transfer (Thomas et al., 2004); R75W and W44C almost completely blocked the electrical coupling of co-expressed WT Cx26 in paired *Xenopus* oocytes, while the recessive mutant W77R did not (Richard et al., 1998; Rouan et al., 2001). Because these mutants did not cause trafficking defect, the dominant effects likely involve improper docking or abnormal gating of the heteromeric heterotypic channels formed. Four mutations (R143Q, D179N, R184Q and C202F) we studied had not been investigated previously.

Eight out of nine mutants markedly diminished calcein transfer of WT Cx26, while they differ in their ability to act as dominant negatives in Cx30 function (Yum et al., 2010). This is significant, since it has previously been assumed that mutant Cx26 would have the same

effect on WT Cx26 and WT Cx30. These mutations result in different severity of hearing loss; whether the variable dominant effects of individual mutants on Cx30 account for the differences remains to be determined.

Of particular interest is the D179N mutant that only partially inhibited dye transfer of Cx26 and did not affect dye transfer of Cx30 (Yum et al., 2010). This is likely a unique functional consequence of the mutation as obvious differences in the transfection efficiency or heteromeric association (as shown in Fig. 1 and Fig 2) has not been observed as compared to other mutants / WT combination. D179N mutation occurs in the highly conserved residue in the second extracellular loop of Cx26 that is shown to mediate inter-connexon interaction (Maeda et al., 2009). It was identified in a family with four affected members presenting mild-to-moderate post-lingual hearing loss (Primignani et al., 2003); whether the partially functional channels account for the milder phenotype in this family, and whether a more severe dominant effect can be demonstrated with other functional assays remain to be determined.

How do dominant GJB2 mutations cause hearing loss?

Haplotype insufficiency could not be the disease mechanism for dominant *GJB2* mutations because individuals heterozygous for recessive *GJB2* deafness mutations do not have impaired hearing. Therefore, dominant mutants that result in hearing loss must have a gain of toxic function. There are likely different types of dominant effects. Some Cx26 mutations associated with keratitis-ichthyosis-deafness syndrome cause cell death that was speculated to be due to aberrant hemichannel activity (Gerido et al., 2007; Lee et al., 2009; Stong et al., 2006). However, this has not been demonstrated in dominant mutations associated with NSHL or SHL with milder forms of skin diseases, and some of these mutants have been shown to increase cell survival instead (Common et al., 2004). Some dominant Cx26 mutants were shown to interfere with trafficking of the co-expressed WT Cx26 and/or Cx30 (Bakirtzis et al., 2003; Shurman et al., 2005). Our data and those of others (Chen et al., 2005; Marziano et al., 2003; Oshima et al., 2003; Piazza et al., 2005; Rouan et al., 2001; Yum et al., 2010) demonstrate that many dominant Cx26 mutants that cause NSHL or SHL with PKK form gap junction plaques with WT Cx26 or Cx30, but the heteromeric/heterotypic channels formed have severely impaired function, likely due to improper docking or defective gating. In this scenario, dominant Cx26 mutants affect hearing by diminishing the function of co-expressed WT Cx26 and/or Cx30, although separating these two effects would require a full understanding of the roles of Cx26 and Cx30 in the cochlea.

Gene deletions in mice demonstrate that both Cx26 and Cx30 are required for hearing (Cohen-Salmon et al., 2002; Teubner et al., 2003), but the roles of Cx26 and Cx30 in cochlea have yet to be fully elucidated. It has been proposed that GJs are involved in ionic coupling, allowing endolymphatic K^+ recycling and the generation of endocochlear potential after the onset of hearing (Wangemann, 2002), but this has not been directly demonstrated. Because both homotypic Cx26 and homotypic Cx30 channels are permeable to K^+ (Manthey et al., 2001; Valiunas et al., 1999), the finding that Cx26 and Cx30 do not compensate for each other in these animal models suggests that K^+ recycling is not the sole role of GJs in the cochlea. Furthermore, this hypothesis would not explain the findings of altered postnatal maturation and development of the organ of Corti before the onset of hearing in conditional *Gjb2*-null mice (Wang et al., 2009) and in a transgenic mouse model expressing a dominant-negative R75W mutant (Inoshita et al., 2008). Emerging evidence supports the idea that GJs mediate metabolic coupling in the cochlea, allowing the exchange of larger molecules such as metabolites, second messengers and glucose (Beltramello et al., 2005; Chang et al., 2008; Zhang et al., 2005). The co-assembly of Cx26 mutants and Cx26 or Cx30 may affect the cellular energy supply and biochemical homeostasis in the cochlea, resulting in hearing loss.

Supplementary Material

Refer to Web version on PubMed Central for supplementary material.

Acknowledgments

We thank Dr. Bruce Nicholson for providing the human *GJB2* cDNA, Dr. Klaus Willecke for the HeLa cells, Dr. Hajime Takano for his advice for the FRAP experiments, Christine Boone, Julia Beamesderfer and Sara Sunshine for technical assistance, and Jennifer Faerber and Dr. Tom Tenhave for statistical analysis. This work was supported by NIH grants KO8 DC005394 (to S.W.Y.), RO1 NS55284 (to S.S.S.), and subcontract and NIH P30 NS047321, which supports the Center for Dynamic Imaging of Nervous System Function, where the FRAP experiments were performed.

REFERENCES

Ahmad S, Chen SP, Sun JJ, Lin X. Connexins 26 and 30 are co-assembled to form gap junctions in the cochlea of mice. Biochemical and biophysical research communications. 2003; 307:362–368. [PubMed: 12859965]

Bakirtzis G, Choudhry R, Aasen T, Shore L, Brown K, Bryson S, Forrow S, Tetley L, Finbow M, Greenhalgh D, Hodgins M. Targeted epidermal expression of mutant Connexin 26(D66H) mimics true Vohwinkel syndrome and provides a model for the pathogenesis of dominant connexin disorders. Human molecular genetics. 2003; 12:1737–1744. [PubMed: 12837696]

Beltramello M, Piazza V, Bukauskas FF, Pozzan T, Mammano F. Impaired permeability to Ins(1,4,5)P_3 in a mutant connexin underlies recessive hereditary deafness. Nat Cell Biol. 2005; 7:63–69. [PubMed: 15592461]

Bruzzone R, White TW, Paul DL. Connections with connexins: the molecular basis of direct intercellular signaling. Eur. J. Biochem. 1996; 238:1–27. [PubMed: 8665925]

Bukauskas FF, Bukauskiene A, Bennett MV, Verselis VK. Gating properties of gap junction channels assembled from connexin43 and connexin43 fused with green fluorescent protein. Biophysical journal. 2001; 81:137–152. [PubMed: 11423402]

Chang Q, Tang W, Ahmad S, Zhou B, Lin X. Gap junction mediated intercellular metabolite transfer in the cochlea is compromised in connexin30 null mice. PLoS ONE. 2008; 3:e4088. [PubMed: 19116647]

Chen YY, Deng YQ, Bao XY, Reuss L, Altenberg GA. Mechanism of the defect in gap-junctional communication by expression of a connexin 26 mutant associated with dominant deafness. Faseb J. 2005; 19:U587–U602.

Cohen-Salmon M, Ott T, Michel V, Hardelin JP, Perfettini I, Eybalin M, Wu T, Marcus DC, Wangemann P, Willecke K, Petit C. Targeted ablation of connexin26 in the inner ear epithelial gap junction network causes hearing impairment and cell death. Curr. Biol. 2002; 12:1106–1111. [PubMed: 12121617]

Common JEA, Di WL, Davies D, Kelsell DP. Further evidence for heterozygote advantage of GJB2 deafness mutations: a link with cell survival. Journal of medical genetics. 2004; 41:573–575. [PubMed: 15235031]

Estivill X, Fortina P, Surrey S, Rabionet R, Melchionda S, D'Agruma L, Mansfield E, Rappaport E, Govea N, Mila M, Zelante L, Gasparini P. Connexin-26 mutations in sporadic and inherited sensorineural deafness. Lancet. 1998; 351:394–398. [PubMed: 9482292]

Forge A, Becker D, Casalotti S, Edwards J, Marziano N, Nickel R. Connexins and gap junctions in the inner ear. Audiol Neuro Otol. 2002; 7:141–145.

Gemel J, Valiunas V, Brink PR, Beyer EC. Connexin43 and connexin26 form gap junctions, but not heteromeric channels in co-expressing cells. Journal of cell science. 2004; 117:2469–2480. [PubMed: 15128867]

Gerido DA, DeRosa AM, Richard G, White TW. Aberrant hemichannel properties of Cx26 mutations causing skin disease and deafness. American journal of physiology. 2007; 293:C337–C345. [PubMed: 17428836]

Grifa A, Wagner CA, D'Ambrosio L, Melchionda S, Bernardi F, Lopez-Bigas N, Rabionet R, Arbones M, Della Monica M, Estivill X, Zelante L, Lang F, Gasparini P. Mutations in GJB6 cause nonsyndromic autosomal dominant deafness at DFNA3 locus. Nat. Genet. 1999; 23:16–18. [PubMed: 10471490]

Harris AL. Emerging issues of connexin channels: biophysics fills the gap. Quarterly reviews of biophysics. 2001; 34:325–472. [PubMed: 11838236]

Inoshita A, Iizuka T, Okamura HO, Minekawa A, Kojima K, Furukawa M, Kusunoki T, Ikeda K. Postnatal development of the organ of Corti in dominant-negative Gjb2 transgenic mice. Neuroscience. 2008; 156:1039–1047. [PubMed: 18793701]

Jagger DJ, Forge A. Compartmentalized and signal-selective gap junctional coupling in the hearing cochlea. J Neurosci. 2006; 26:1260–1268. [PubMed: 16436613]

Kelsell DP, Dunlop J, Stevens HP, Lench NJ, Liang JN, Parry G, Mueller RF, Leigh IM. Connexin 26 mutations in hereditary non-syndromic sensorineural deafness. Nature. 1997; 387:80–83. [PubMed: 9139825]

Kikuchi T, Kimura RS, Paul DL, Adams JC. Gap junctions in the rat cochlea: immunohistochemical and ultrastructural analysis. Anat. Embryol. 1995; 191:101–118. [PubMed: 7726389]

Kumar NM, Gilula NB. The gap junction communication channel. Cell. 1996; 84:381–389. [PubMed: 8608591]

Lautermann J, tenCate WJF, Altenhoff P, Grummer R, Traub O, Frank HG, Jahnke K, Winterhager E. Expression of the gap-junction connexins 26 and 30 in the rat cochlea. Cell and tissue research. 1998; 294:415–420. [PubMed: 9799458]

Lee JR, Derosa AM, White TW. Connexin mutations causing skin disease and deafness increase hemichannel activity and cell death when expressed in Xenopus oocytes. The Journal of investigative dermatology. 2009; 129:870–878. [PubMed: 18987669]

Maeda S, Nakagawa S, Suga M, Yamashita E, Oshima A, Fujiyoshi Y, Tsukihara T. Structure of the connexin 26 gap junction channel at 3.5 A resolution. Nature. 2009; 458:597–602. [PubMed: 19340074]

Manthey D, Banach K, Desplantez T, Lee CG, Kozak CA, Traub O, Weingart R, Willecke K. Intracellular domains of mouse connexin26 and-30 affect diffusional and electrical properties of gap junction channels. J Membrane Biol. 2001; 181:137–148. [PubMed: 11420600]

Marziano NK, Casalotti SO, Portelli AE, Becker DL, Forge A. Mutations in the gene for connexin 26 (GJB2) that cause hearing loss have a dominant negative effect on connexin 30. Human molecular genetics. 2003; 12:805–812. [PubMed: 12668604]

Orthmann-Murphy JL, Freidin M, Fischer E, Scherer SS, Abrams CK. Two distinct heterotypic channels mediate gap junction coupling between astrocyte and oligodendrocyte connexins. J Neurosci. 2007; 27:13949–13957. [PubMed: 18094232]

Oshima A, Doi T, Mitsuoka K, Maeda S, Fujiyoshi Y. Roles of Met-34, Cys-64, and Arg-75 in the assembly of human connexin 26 - Implication for key amino acid residues for channel formation and function. J. Biol. Chem. 2003; 278:1807–1816. [PubMed: 12384501]

Piazza V, Beltramello M, Menniti M, Colao E, Malatesta P, Argento R, Chiarella G, Gallo LV, Catalano M, Perrotti N, Mammano F, Cassandro E. Functional analysis of R75Q mutation in the gene coding for Connexin 26 identified in a family with nonsyndromic hearing loss. Clin Genet. 2005; 68:161–166. [PubMed: 15996214]

Primignani P, Castorina P, Sironi F, Curcio C, Ambrosetti U, Coviello DA. A novel dominant missense mutation - D179N - in the GJB2 gene (Connexin 26) associated with non-syndromic hearing loss. Clin Genet. 2003; 63:516–521. [PubMed: 12786758]

Richard G, White TW, Smith LE, Bailey RA, Compton JG, Paul DL, Bale SJ. Functional defects of Cx26 resulting from a heterozygous missense mutation in a family with dominant deaf-mutism and palmoplantar keratoderma. Human genetics. 1998; 103:393–399. [PubMed: 9856479]

Rouan F, White TW, Brown N, Taylor AV, Lucke TW, Paul DL, Munro CS, Uitto J, Hodgins MB, Richard G. Trans-dominant inhibition of connexin-43 by mutant connexin-26: implications for dominant connexin disorders affecting epidermal differentiation. J Cell Sci. 2001; 114:2105–2113. [PubMed: 11493646]

Shurman DL, Glazewski L, Gumpert A, Zieske JD, Richard G. In vivo and in vitro expression of connexins in the human corneal epithelium. Investigative ophthalmology & visual science. 2005; 46:1957–1965. [PubMed: 15914609]

Stong BC, Chang Q, Ahmad S, Lin X. A novel mechanism for connexin 26 mutation linked deafness: cell death caused by leaky gap junction hemichannels. The Laryngoscope. 2006; 116:2205–2210. [PubMed: 17146396]

Su CC, Li SY, Su MC, Chen WC, Yang JJ. Mutation R184Q of connexin 26 in hearing loss patients has a dominant-negative effect on connexin 26 and connexin 30. Eur J Hum Genet. 18:1061–1064. [PubMed: 20442751]

Sullivan R, Lo CW. Expression of a connexin 43/beta-galactosidase fusion protein inhibits gap junctional communication in NIH3T3 cells. The Journal of cell biology. 1995; 130:419–429. [PubMed: 7542247]

Sun JJ, Ahmad S, Chen SP, Tang WX, Zhang YP, Chen P, Lin X. Cochlear gap junctions coassembled from Cx26 and 30 show faster intercellular Ca^{2+} signaling than homomeric counterparts. Amer J Physiol Cell Physiol. 2005; 288:C613–C623. [PubMed: 15692151]

Teubner B, Michel V, Pesch J, Lautermann J, CohenSalmon M, Sohl G, Jahnke K, Winterhager E, Herberhold C, Hardelin JP, Petit C, Willecke K. Connexin30 (Gjb6)-deficiency causes severe hearing impairment and lack of endocochlear potential. Hum. Mol. Genet. 2003; 12:13–21. [PubMed: 12490528]

Thomas T, Shao Q, Laird DW. Differentiation of organotypic epidermis in the presence of skin disease-linked dominant-negative Cx26 mutants and knockdown Cx26. The Journal of membrane biology. 2007; 217:93–104. [PubMed: 17638039]

Thomas T, Telford D, Laird DW. Functional domain mapping and selective trans-dominant effects exhibited by Cx26 disease-causing mutations. J. Biol. Chem. 2004; 279:19157–19168. [PubMed: 14978038]

Valiunas V, Manthey D, Vogel R, Willecke K, Weingart R. Biophysical properties of mouse connexin30 gap junction channels studied in transfected human HeLa cells. The Journal of physiology. 1999; 519(Pt 3):631–644. [PubMed: 10457079]

Wang Y, Chang Q, Tang W, Sun Y, Zhou B, Li H, Lin X. Targeted connexin26 ablation arrests postnatal development of the organ of Corti. Biochemical and biophysical research communications. 2009; 385:33–37. [PubMed: 19433060]

Wangemann P. K+ cycling and the endocochlear potential. Hearing research. 2002; 165:1–9. [PubMed: 12031509]

White TW, Bruzzone R. Multiple connexin proteins in single intercellular channels: connexin compatibility and functional consequences. J. Bioenerg. Biomembranes. 1996; 28:339–350.

Willecke K, Eiberger J, Degen J, Eckardt D, Romualdi A, Guldenagel M, Deutsch U, Söhl G. Structural and functional diversity of connexin genes in the mouse and human genome. Biol. Chem. 2002; 383:725–737. [PubMed: 12108537]

Xia JH, Liu CY, Tang BS, Pan Q, Huang L, Dai HP, Zhang BR, Xie W, Hu DX, Zheng D, Shi XL, Wang DA, Xia K, Yu KP, Liao XD, Feng Y, Yang YF, Xiao JY, Xie DH, Huang JZ. Mutations in the gene encoding gap junction protein β-3 associated with autosomal dominant hearing impairment. Nat. Genet. 1998; 20:370–373. [PubMed: 9843210]

Yum SW, Zhang J, Scherer SS. Dominant connexin26 mutants associated with human hearing loss have trans-dominant effects on connexin30. Neurobiology of disease. 2010

Yum SW, Zhang J, Valiunas V, Kanaporis G, Brink PR, White TW, Scherer SS. Human connexin26 and connexin30 form functional heteromeric and heterotypic channels. American journal of physiology. 2007; 293:C1032–C1048. [PubMed: 17615163]

Zhang Y, Tang W, Ahmad S, Sipp JA, Chen P, Lin X. Gap junction-mediated intercellular biochemical coupling in cochlear supporting cells is required for normal cochlear functions. Proceedings of the National Academy of Sciences of the United States of America. 2005; 102:15201–15206. [PubMed: 16217030]

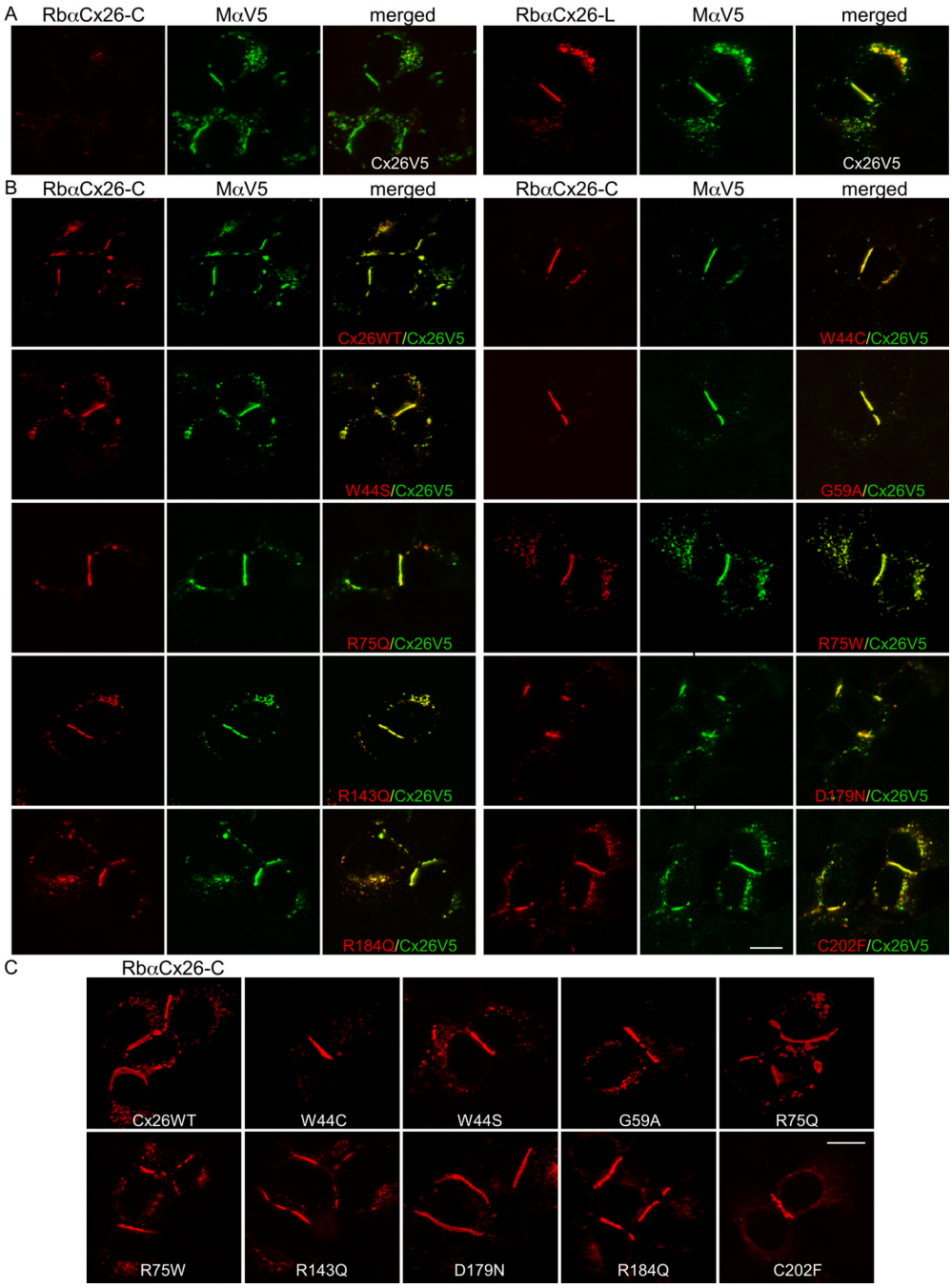

Figure 1. Dominant Cx26 mutants co-localize with WT Cx26 at gap junction plaques

These are confocal images of transiently transfected HeLa cells that express WT Cx26 with a C-terminal V5 epitope tag (Cx26V5) alone (A), or co-express Cx26V5 and WT Cx26 (Cx26WT) or the indicated Cx26 mutants (B), or the individual Cx26 mutants alone as indicated (C) (A) These cells were co-labeled with a mouse antibody against V5 (MaV5) and a rabbit antiserum against the C-terminus (RbaCx26-C, left panel) or the cytoplasmic loop (RbaCx26-L, right panel) of Cx26. Note that the V5 tag did not alter the trafficking of Cx26V5 to gap junction plaques at apposed cell borders as visualized with MaV5 or RbaCx26-L (right panel), whereas the immunoreactivity to the RbaCx26-C was minimal and

never seen at the gap junction plaques (left panel), indicating that the V5 tag prevented the binding of the RbaCx26-C antiserum.
(B) These cells were co-labeled with RbaCx26-C (to visualize the untagged WT or mutant Cx26) and MaV5 (to visualize Cx26V5). Similar to Cx26WT, all of these Cx26 mutants were colocalized with Cx26V5, including at gap junction plaques. Scale bar: 10 μm. (C) These are confocal images of HeLa cells transiently transfected to express WT Cx26 (Cx26WT) or the indicated Cx26 mutants. The cells were labeled with a rabbit antiserum against the C-terminus of Cx26. Similar to the WT Cx26, all of these mutants formed gap junction plaques at apposed cell borders. Scale bar: 10 μm.

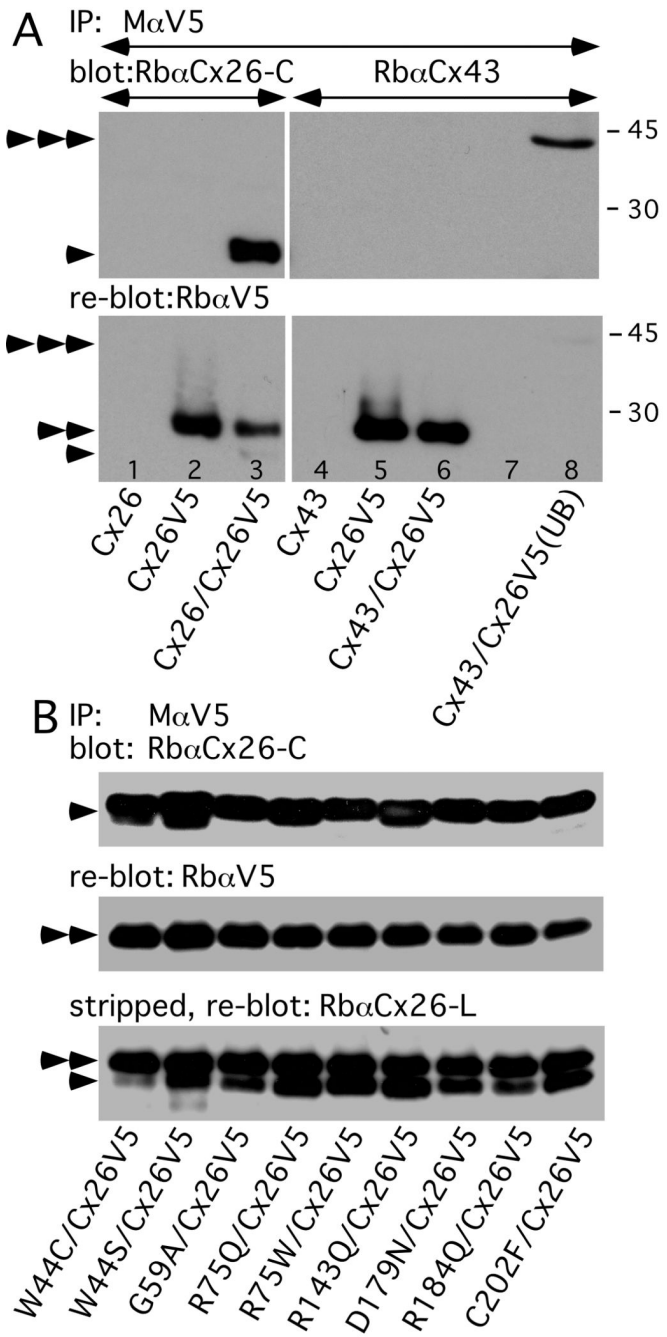

Figure 2. Cx26V5 co-immunoprecipitates dominant Cx26 mutants

(A) HeLa cells were transiently transfected to express WT Cx26, Cx26V5, or both Cx26V5 and WT Cx26, as well as WT Cx43, Cx26V5, or both WT Cx43 and Cx26V5. Lysates were immunoprecipitated (IP) with a mouse monoclonal antibody against V5 (MαV5), probed with a rabbit antiserum against the C-terminus of Cx26 (RbαCx26-C, lanes 1–3) or Cx43 (RbαCx43, lanes 4–8), then reprobed with a rabbit antiserum against V5 (RbαV5). Note that the MαV5 co-immunoprecipitated Cx26 (lane 3), but did not co-immunoprecipitate Cx43 (lane 6), which is present in the unbound fraction (UB) of the lysate (lane 8). Because the blot was not stripped before reprobing, faint signals for Cx26 (arrowhead) and Cx43 (triple arrowhead) are present.

(B) HeLa cells were transfected to co-express Cx26V5 and one of the indicated Cx26 mutants. Lysates were immunoprecipitated with MαV5, probed with RbαCx26-C (upper panel), reprobed with RbαV5 (middle panel), then stripped and reprobed again with a rabbit antiserum against the cytoplasmic loop of Cx26 (RbαCx26-L, lower panel). Note that MαV5 co-immunoprecipitates Cx26 mutants in all cases, as shown by the bands in the upper panel and by the lower set of bands in the lower panel. The untagged Cx26 (single arrowhead) ran slightly further in the gel than did the Cx26V5 (double arrowheads). Size markers (in kDa) are shown.

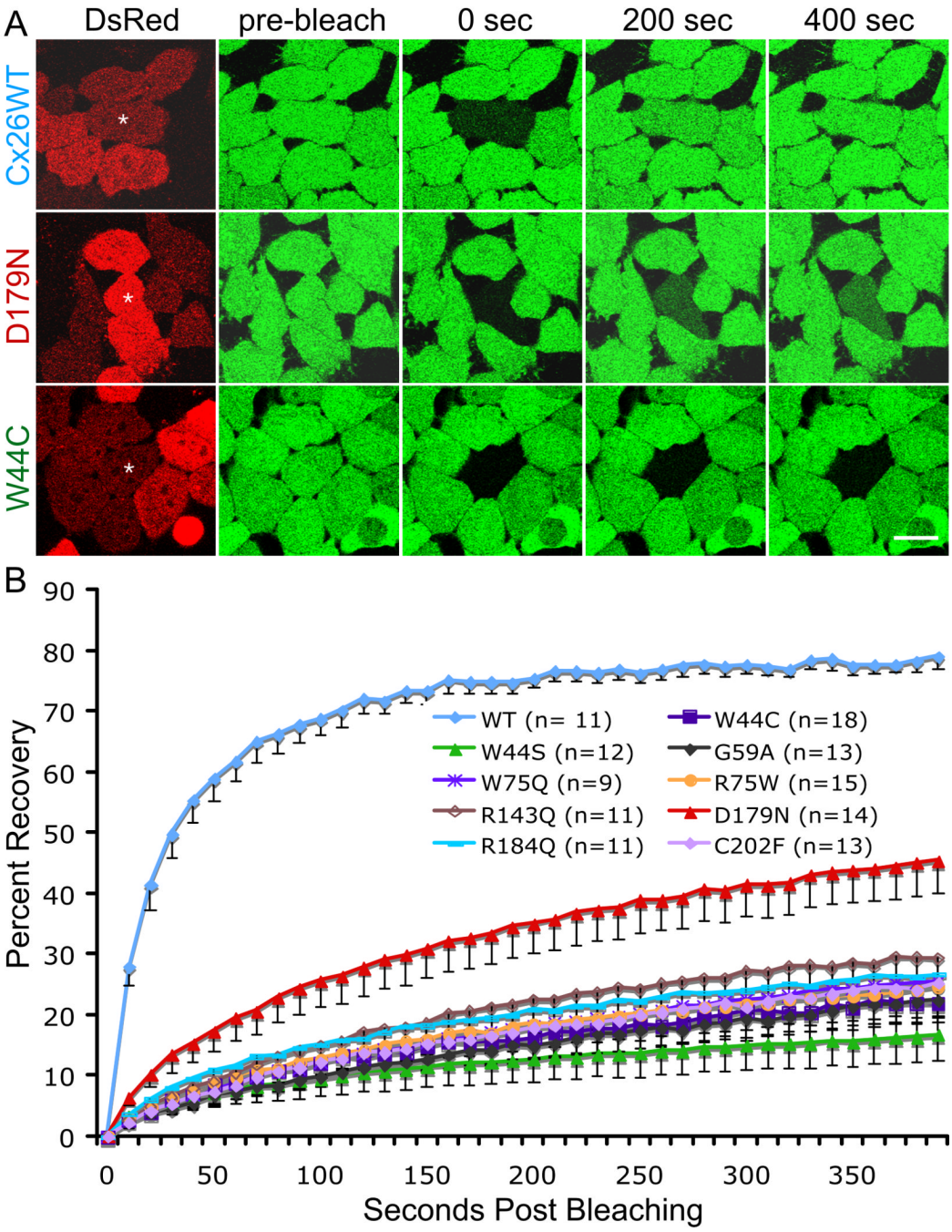

Figure 3. Dominant Cx26 mutants inhibited dye transfer of cells stably expressing WT Cx26

FRAP was performed in HeLa cells stably expressing Cx26 that were transiently transfected to express WT Cx26 (Cx26WT) or one of nine individual different dominant Cx26 mutants (in a DsRed bicistronic vector) as indicated. Two days later, the cells were incubated in calcein AM to fill the cytoplasm with calcein (green), and selected, single cells expressing DsRed (red) that were in close contact with at least four other DsRed-positive cells were photobleached, and then the green fluorescence signal was measured every 10 sec for 400 sec.

(A) Examples of cells immediately before (pre-bleach), immediately after (0 sec), 200 seconds and 400 seconds after bleaching. An asterisk (*) indicates the cell selected for bleaching. Scale bar: 10 μm.
(B) Summary of the FRAP data for many individual cells. For every bleached cell, the fluorescent signal present in each cell immediately prior to and immediately after photobleaching was normally to 100% and 0%, respectively. The number of pooled cells is indicated in parentheses. For each mutation, the curves connect the mean percent recovery at each time point; the vertical bars represent means ± SE. Note that the recovery of the calcein signal in the bleached cells co-expressing the 9 individual mutants was significantly less than that in cells co-expressing Cx26WT ($p < 0.0001$).